1st International Conference on Advances in Science, Engineering and Robotics Technology 2019 (ICASERT 2019)

# Offshore Wind Energy Estimation in the Bay of Bengal with Satellite Wind Measurement

Navila Rahman Nadi
*Lecturer,Dept. of EEE*
*Independent University, Bangladesh.*
Dhaka, Bangladesh.
navila@iub.edu.bd

Ferhat Bingöl
*Assist. Prof. ,Energy Systems Engineering*
*Izmir Institute of Technology*
Izmir, Turkey
ferhatbingol@iyte.edu.tr

Merete Badger
*Senior Scientist, Dept. of Wind Energy, Technical University of Denmark(DTU)*
Roskilde, Denmark
mebc@dtu.dk

***Abstract*— The objective of this paper is to obtain appropriate offshore location in the Bay of Bengal, Bangladesh for further development of wind energy. Through analyzing the previous published works, no offshore wind energy estimation has been found related to the Bay of Bengal. Therefore, this study can be claimed as the first footstep towards offshore wind energy analysis for this region. Generally, it is difficult to find offshore wind data relative to the wind turbine hub heights, thus a starting point is necessary to identify the possible wind power density of the region. In such scenario, Synthetic Aperture radars (SAR) have proven useful in previous studies. In this study, SAR based dataset- ENVISAT ASAR has been used for Wind Atlas generation of the Bay of Bengal. Furthermore, a comparative study has been performed with Global Wind Atlas (GWA) to determine a potential offshore wind farm production in a reasonable location at the bay. The annual energy production of that offshore windfarm has been analyzed by combining SAR, GWA and ASCAT datasets. Through ASAR based Wind Atlas and GWA comparison, some differences have been found where there are less samples from the ASAR datasets. Thus, Weibull statistical analysis are performed to have a better Weibull fitting and accurate estimation of Annual Energy production (AEP). The study summarizes that, satellite datasets can be a very useful method to detect potential zone if compared with any long time statistical result and bathymetry data together.**

***Keywords*— *Wind Atlas, Satellite wind measurements, Weibull distribution, ASCAT, ASAR, Offshore***

## I. INTRODUCTION

Increasing demand of offshore wind parks in various countries has promoted wind resource mapping over the sea. The original method to estimate the wind energy resource is by installing a meteorological mast at one or more specific sites for minimum one year. This mostly requires more time as well as becomes costly and this drawback leads to search of another alternative method which gives indications of wind resources and help in proper decision making of feasibility studies for the prospective wind parks. In such scenario, satellite remote sensing is useful. Execution of these satellite based images in order to derive wind speed in the early stages of wind farm planning is becoming praiseworthy because of its spatial and time coverage along with cost effectiveness [1]. This useful method can predict perfect area of higher wind resources which leads to the planning of feasibility studies and provide a faithful supplement to the traditional assessments [3].

The main study area is chosen as the Bay of Bengal, which is considered as the largest Bay of the world which comprises around 2090 km of length and 1610 km of width. The total surface area of Bay of Bengal is around 2 million km$^2$ and it is bounded by Sri Lanka and India in the west side, Myanmar and Andaman and Nicobar islands in the east side and Bangladesh in the North side. It has a high depth of around 5 km and average depth of 2600 m which can be an impeccable study area for offshore floating wind turbines [2]. Broad wind analysis has not been performed yet in this bay to find out the wind energy resources, only few studies have been done in the Indian coasts which just covers a specific western zone of the Bay of Bengal. Also, no wind atlas generation for larger domain and wind energy estimation has been performed in the Bay of Bengal which is the main concentration of this paper.

In our study, the obtained datasets were compared with the Global Wind Atlas (GWA) datasets. GWA provides long-term high resolution wind climatology at 50, 100, 200m hub heights for the whole world including onshore and 30 km from offshore as a free access online [12]. This wind atlas provides wind resource data at 1 km resolution and contains data at a higher spatial resolution of 250 m [12]. The information provided in the Atlas along with further specific regional studies, supports to identify the prospective areas for additional preliminary assessment of technical possibilities.

## II. SATELLITE TECHNOLOGIES FOR OFFSHORE WIND

In this paper, two types of satellites were analyzed which are: Synthetic Aperture Radar (SAR) and Scatterometer. The studied datasets were attained from SAR methodology based Advanced Synthetic Aperture Radar (ENVISAT ASAR) and from Advanced Scatterometer (ASCAT) satellites.

### *A. Synthetic Aperture Radar (SAR) technology*

SAR is a remote sensing technique which transmits microwave pulses of energy to illuminate an area of the Earth surface. The pulses gets scattered because of the surface properties and a portion returns to the instrument with a change in amplitude, polarization, travel time and phase [3]. All these backscattered signals for each foot print area stores in the satellite to process a two dimensional image of the surface. SAR has higher spatial resolution (around 1km) and preferred more for coastal wind energy measurements [5].The data acquisition from the SAR pulses can be performed in day or night even if it is cloudy or light rainy (Christiansen, 2006). SAR signals are electromagnetic waves with a polarization determined by the orientation of the electric field [3]. Some upgraded SAR systems have the capability of transmitting and receiving both polarization simultaneously, and deliver quad observable SAR images [4].

978-1-7281-3445-1/19/$31.00 ©2019 IEEE

ENVISAT ASAR (Environmental satellite based Advanced Synthetic Aperture Radar) satellite is based on SAR technology and it is actually an Environmental satellite capable of scanning the surface in one of the four polarization combinations. [4]. The mission was later followed up by the Sentinel-1 A/B mission. It is being established by European Space Agency (ESA) in 1 March,2002 until 9 May, 2012, when ESA lost the contact with the satellite [5]. The satellite take images and send to the base station down in earth to preserve. The spatial resolution of the images is around 150 m and swath mode around 400 km. The total incidence angle coverage is 15-45 degree [3] . In the scenario of ocean winds, the average of around 1km resolution is processed for SAR images in a purpose to lessen the natural speckle noise and modulation error [9]. In WSM (wide swath mode) of SAR data acquisition, it can map a point at mid-latitude (55°N) around 15 times per month [9]. The ENVISAT ASAR dataset is freely accessible from the European Space Agency (ESA) archive from where the required data can be downloaded and used for further scientific research studies.

### *B. Scattterometer Technology*

Scatterometer is a real aperture radar that also uses microwave technology are sun – synchronous polar orbiting satellites similar to SAR. These kind of satellites have a fixed local time of observations for ascending and descending mode. Scatterometers operate in the radar scale of C-band (around 5 GHz) or in Ku-band (around 13 GHz)[5]. One of the prime differences in between Scatterometer and SAR is that, Scatterometters take multiple (3 to 4) views of the surface from the antennae while SAR takes only one directional view. Due to this higher area coverage capability Scatterometer's observation rate is higher than SAR [5].

In October 2006 the Advanced Scatterometer (ASCAT) was launched on the EUMETSAT (European Organization for the Exploitation of Meteorological Satellites) MetOp-A which is Meteorological Operational satellite program (MetOp) and became completely operational from May, 2007 until today [6]. From September 2012, MetOp-B became operative, whereas both of these satellites has same ASCAT instruments. Being a C-Band Scatterometer, ASCAT operates two times a day (day and night) through its 3 vertically polarized antennas transmitting pulses at 5.255 GHz [7]. ASCAT has a double swath as the fan-beam antennae is slanted towards 45, 90, and 135° with satellite track where the extended side of antennae possesses two swaths each consisting of 550 Km wide separated by a gap of about 670 Km nadir gap. [14] Having two swaths ASCAT can provide mapping of all locations at a midpoint (55°N) around 40 times per month [9]. Comparing with ENVISAT ASAR it has more frequent imaging as ASAR maps 15 times per month for the same midpoint.

## III. DATA ANALYSIS OF THE BAY OF BENGAL

The fundamental of this paper is to create a wind atlas for the Bay of Bengal by using ENVISAT ASAR datasets and through a comparative analysis with Global Wind Atlas (GWA), finding a suitable location for wind farm estimation. In this paper, the wind atlas methodology has been followed to create a wind atlas. This step by step process has been displayed in a flow chart below. The interest area of our study locates in UTM 45N zone, at 82° to 95° Eastern longitude and 16.5° to 23° Northern latitude.

### *A. ASAR datasets*

The Bay of Bengal has been mapped through ASAR on-board by European Space Agency satellite ENVISAT from 2006 until 2012. A total number of 466 Wide Swath Mode (WSM) scenes from 2002 until 2012 are collected from the ESA's ordering system EOLI-SA (Earth Observation Link) with special request by DTU. Each of those WSM scenes cover 400 x 400 km.

After receiving the WSM scenes, the wind retrieval offshore wind maps were produced. This whole process of the wind retrieval is done with a patented software called by ANSWRS (Applied Physics Laboratory National Oceanic and Atmospheric Administration (NOAA) SAR Wind Retrieval System)[3]. ANSWRS is a well effective software for wind retrieval from the ASAR WSM scenes which has been used in all previous SAR based offshore wind atlas generation [3] [8][9] [10] [11]. The SAR wind directional data was attained at 1 degree latitude and longitude resolution from the US Navy Operational Global Atmospheric Prediction System (NOGAPS)[5]. NOGAPS is modeled as 6-hourly wind direction provider which were interpolated spatially to be suitable for usage with the SAR images as previously it has been mentioned that, SAR only takes one directional images. So it cannot detect the wind direction by itself. For geophysical model function CMOD-5.n is being used. CMOD-5.n is an updated version of the CMOD5 which provides neutral condition of wind speed at 10m [5]. In the below Figure 2, it represents two ENVISAT ASAR WSM wind scenes on the date of 26 June, 2010 and 9 March 2009 respectively in ascending and descending formats.

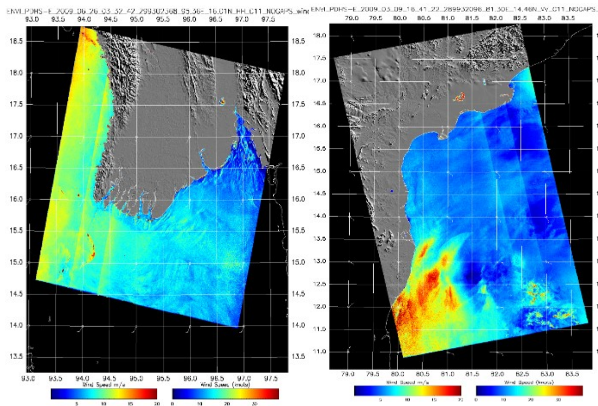

Figure 1: ENVISAT ASAR retrieved wind scenes of 26 June 2010 and 9 March 2009 at 16.41:22 and at 03.32:42 UTC in the Bay of Bengal accordingly.

The satellite wind retrieved fields received from the DTU were merged and combined for wind resource mapping using the DTU Wind tool S-WAsP. In S-WAsP, a second moment fitting for the Weibull scale (A) and shape (k) parameters are used to fit a distribution to all data and estimate the two Weibull parameters.

## B. ASCAT datasets

In this study, the similar way, ASCAT datasets has been received and further retrieved to achieve wind scenes for that specific location. National Oceanic and Atmospheric Administration (NOAA)'s weather forecasting and warning mission operationally supports the production and utilization of ASCAT ocean surface vector wind products [15]. Royal Netherlands Meteorological Institute (KINMI) has developed the ASCAT wind data processor for the standard ASCAT wind by using GMF CMOD5.N [15]. KNMI produces the gridded version (cell size of 12.5 km) product of ASCAT wind speed and direction within EUMETSAT OSI SAF. (SAF, 2013). In our study, ASCAT observations are extracted from the ASCAT Level 3 Coastal Ocean Surface Wind Vector product (MyOcean). L3 daily gridded wind product is available from the MyOcean catalogue after registration at their site for the defined location.

## C. GWA datasets

For this paper, the global wind dataset were collected in modern Era-Retrospective Analysis for Research and Applications (MERRA) format from the free access internet as .lib files for definite co-ordinates and then matched those nodal points with the obtained SAR data locations. In the concerned area, the sample nodal locations of SAR .lib files were matched with the downloaded GWA location defined .lib files for 10m height.

# IV. Statistical analysis

For analyzing the wind speed data, the two parameter Weibull Probability distribution function (PDF) is most appropriate and acknowledged. This PDF provides an enhanced fitting to predict high accurate monthly distribution of wind speed. The Weibull Probability function is denoted in [16] as:

$$f(v) = (\frac{k}{A})(\frac{v_i}{A})^{k-1}\exp[-(\frac{v_i}{A})]^k \quad (1)$$

where $f(v)$ is denoted as the probability of observed wind speed, A is the Weibull scale parameter and k is the unit less Weibull shape parameter, $v_i$ is wind speed. The two Weibull parameters and the average wind speed are related by [16]

$$\bar{v} = A.\Gamma\,(1+\frac{1}{k}) \quad (2)$$

By using the Weibull parameters, gamma function Γ and the air density ρ (~1.245 g m−3) the wind power density is predicted in [16] as:

$$E = \frac{1}{2}\rho A_w^3.\Gamma\left(1+\frac{3}{k_w}\right) \quad (3)$$

where $\bar{v}$ is the average wind speed, E is the power density and Γ is the gamma function. In this study, four methods of statistical analysis were compared to determine the shape and scale parameters of Weibull wind speed distribution for wind energy resource analysis, these are:

## A. Empirical Method

Empirical method (EM) is a comparison set using the standard deviation and mean wind speed. It is considered as a distinctive situation of Method of moments (MOM). Through EM the parameters of Weibull distribution can be found from [16] as:

$$k = (\frac{\sigma}{\bar{v}})^{-1.086} \quad (4)$$

$$A = \frac{\bar{v}}{\Gamma\,(1+\frac{1}{k})} \quad (5)$$

where $\bar{v}$ is the average wind speed, $\sigma$ is the standard deviation and Γ is the gamma function.

## B. Method of Moments

In estimating Weibull distribution parameters Method of moments (MOM) is widely used. The equation format is dependent on the arithmetical iteration of mean wind speed ($\bar{v}$) and standard deviations (σ). The equations [16] are followed as:

$$k = (\frac{0.9874}{\frac{\sigma}{\bar{v}}})^{1.0983} \quad (6)$$

$$A = \frac{\bar{v}}{\Gamma\,(1+\frac{1}{k})} \quad (7)$$

where $\bar{v}$ is the average wind speed, $\sigma$ is the standard deviation and Γ is the gamma function.

## C. Method of Moment 3

By Moment 3 method of Weibull parameter estimation, first the k parameter is being determined from [17] through equation 4.12.

$$\frac{\bar{v}^3}{\overline{(v)}^3} = \frac{\Gamma(1+\frac{3}{k})}{\Gamma(1+\frac{1}{k})^3} \quad (8)$$

Afterwards the A parameter is determined from

$$A = \frac{\bar{v}}{\Gamma\,(1+\frac{1}{k})} \quad (9)$$

where $\bar{v}$ is the mean wind speed and Γ is the gamma function

## D. Power Density Method

The power density method (PDM) is a numerical analysis related to the mean wind speed and for this method initially the Energy Pattern Factor ($E_{pf}$) should be computed. $E_{pf}$ can be defined as the ratio of mean of cubic wind speed to the cube of mean wind speed. The energy pattern factor (EPF) denoted in [16] as:

$$E_{pf} = \frac{\frac{1}{N}\sum_{i=1}^{N} {v_i}^3}{(\frac{1}{N}\sum_{i=1}^{N} v_i)^3} \quad (10)$$

Subsequently, the shape parameter (k) and scale parameter (A) can be calculated from the previous $E_{pf}$ equation through below format described in [16] as:

$$k = 1 + \frac{3.69}{{E_{pf}}^2} \quad (11)$$

$$A = \frac{\bar{v}}{\Gamma\,(1+\frac{1}{k})} \quad (12)$$

where $\bar{v}$ is the average wind speed, $v_i$ is the observed hourly wind speed, $E_{pf}$ is the energy pattern factor. With the aim of evaluating the accuracy of the previously mentioned 4 Weibull methods, 3 types of error estimation has been calculated. Those are:

## E. Root Mean Square Error (RMSE)

RMSE estimates the error by considering the deviation between the predicted and the experimental values. The lower the value of RMSE is, the more accurate the values are. RMSE should be as close by to zero as possible to have a successful forecasting of prediction. The equation formula of RMSE is described in [16] as:

$$\text{RMSE} = (\frac{1}{N}\sum_{i=1}^{N}(y_i - x_i)^2)^{1/2} \quad (13)$$

where, $y_i$ is the frequency of the observation , $x_i$ frequency of Weibull ( using those statistical methods) and N is the number of observations.

*F. Chi-Square Test($\chi^2$)*

This test is considered accurate when the value comes closer to zero. Basically it gives back the mean square of the deviations between the experimental and the calculated values for the distributions. Chi-squared test is calculated in [16] as following:

$$\chi^2 = \sum_{i=1}^{N} \frac{(y_i - x_i)^2}{x_i} \quad (14)$$

where, $y_i$ is the frequency of the observation $x_i$ frequency of Weibull ( using those statistical methods) and N is the number of observations.

*G. Coefficient of Determination ( $R^2$)*

The coefficient of determination ( $R^2$) represents a linear relationship between the calculated values and observed data. The higher value of it represents a better fit and the highest value it can get is 1. The function can be represented in [17] as:

$$R^2 = 1 - \frac{SS_{RES}}{SS_{TOT}} \quad (15)$$

$$where,\ SS_{RES} = \sum_{i=1}^{N} (y_i - f_i)^2 \quad (16)$$

$$SS_{TOT} = \sum_{i=1}^{N} (y_i - \bar{y})^2 \quad (17)$$

Here, $y_i$ is the frequency of the observation, $\bar{y}$ is the mean of the observed data, N is the number of observation, $f_i$ is the predicted value.

## V. RESULTS

The purpose of this section is to combine all the satellite datasets to generate a Wind Atlas of the Bay of Bengal and have a comparative study among GWA and satellite datasets.

*H. Wind Atlas Generation*

After S-WAsP mapping of the achieved wind scenes, the time-series wind measurement dataset is being generated as .tab files which is a file format for observed wind climate. From then the forming of a generalized wind climate in .lib file begins which is format of the Atlas files. For this instance, a vector map of the whole zonal area is used for specific terrain analysis and a met-station for the site precise location is settled up in WAsP.

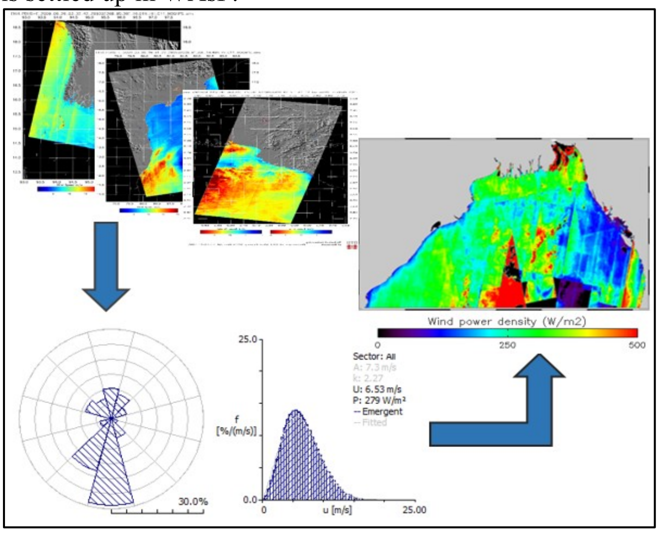


Figure 2: Wind resource mapping process from ASAR wind scenes

If the met station location is preferable and specific under that zonal area, the Generalized Wind Climate can be further calculated. For each .tab file, the same procedure is followed to create the respective .lib files. The generated .lib file contains the sectoral wise frequency of occurrence of the wind (the wind rose) as well as the wind speed frequency distributions in the same sectors (as Weibull A- and k-parameters). The wind climates are specified for a number of reference roughness classes and heights above ground level.

For specific roughness and height selection, it provides a combined 12 sectoral wind rose, sectoral frequencies of the wind direction, mean wind speed, mean power density along with Weibull shape (k) and scale (A) parameters

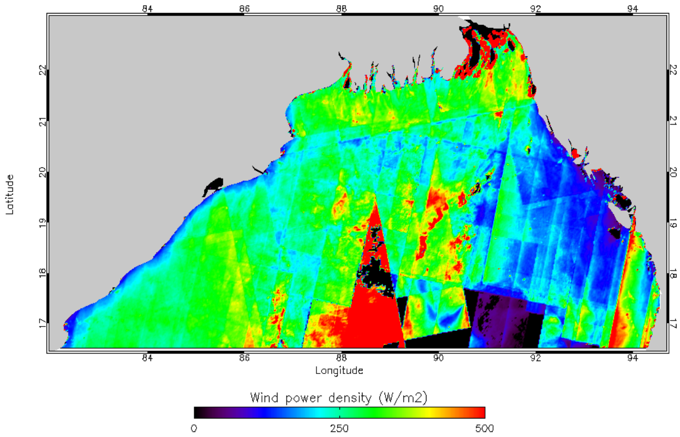


Figure 3: Wind Power density map of the Bay of Bengal through ENVISAT ASAR wind dataset

*B. Comparison and Outcomes*

The nodal comparison was done in an area basis (60 km by 60 km) keeping the GWA node points in the middle. So these area wise nodal comparisons were performed where 122 coordinated nodal location points are found in the defined zone. While comparing the Satellite based Atlas with GWA, we have found in further from shore areas, the number of samples are really scanty which leads to a lower data obtain scenario of that particular area. The higher the number of samples, the better the estimation can be provided. In addition, from previous studies it has been perceived that, wind resources can be predicted well enough through 70 samples considering an uncertainty of ±10% at a confidence level of 90% [13]. To gain more accuracy, those ENVISAT ASAR nodal locations were chosen which has more than 70 time series samples. This lead to 26 nodal sample comparison in between GWA and ENVISAT ASAR wind atlas.

In the figure 4, 5, 6 and 7, the scenes which has more than 70 time series samples has been selected. For this reason other nodal points of deep sea is showing as null values. From the figure, two particular interest areas can be found where the number of samples are moderate, which is in the Northern coastal area near Bangladesh and in the Western side of the Bay of Bengal near India. While comparing the mean wind speed verified ENVISAT ASAR wind Atlas map with GWA, ENVISAT ASAR wind Atlas map shows a moderate result, though the ASAR seems to be over predicting the wind speed and energy entirely, especially in the Northern coastal areas.

In the figure 4, it shows the calculated offshore mean wind speed from ENVISAT ASAR datasets. The color legend shows the variation of mean wind speed availability of that particular zone of the Bay of Bengal. From the legend it is clear that, the color orange to red is the high potential zone whereas the color below are indicating a lower wind speed scenario. Figure 4 represents a variation of around 6-7.5 ms$^{-1}$ mean speed. In the Northern side of the Bay of Bengal, the mean wind speed is around 6.5-7.5 ms$^{-1}$ where as in Eastern part it varies around 6-7.29 ms$^{-1}$ On the other hand, figure 5 represents the GWA mean wind speed for the same location points where GWA shows a variation of wind speed from 5.05 to 7.82 ms$^{-}$ Alike SAR, It can be seen that in Western side of the Bay of Bengal, the mean wind speed is found to be around 6.5-7.2 ms$^{-1}$.

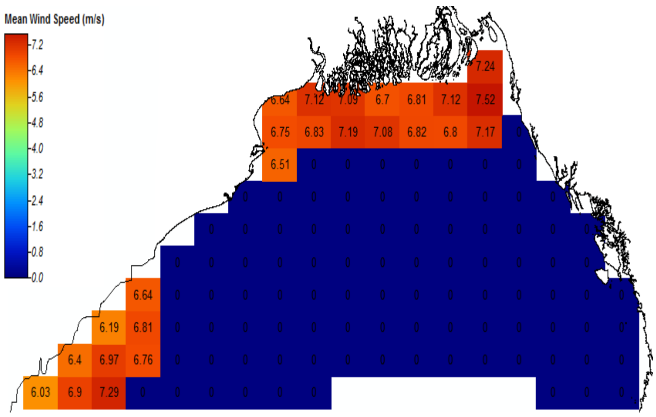


Figure 4 : Mean wind speed of the specified location from ENVISAT ASAR datasets

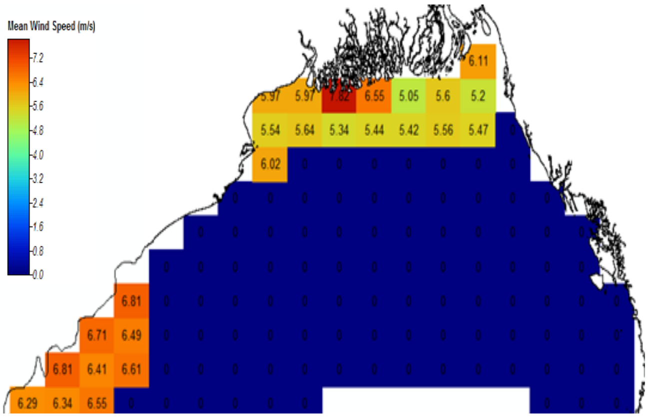


Figure 5 : Mean wind speed of the specified location from GWA datasets

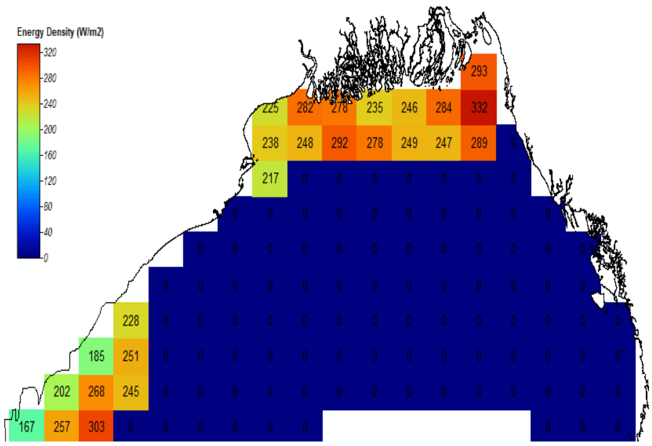


Figure 6. Energy density of the specified location from ENVISAT ASAR datasets.

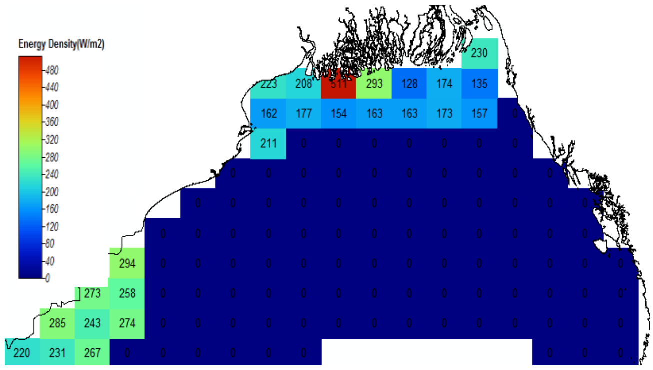


Figure 7. Energy density of the specified location from GWA datasets

Figure 6 represents the energy density from ENVISAT ASAR datasets for the specific location where it shows a good variation of 225-332 W/m2 in near coastal area of Northern side of the Bay of Bengal where as in Western coast it is a bit less comparatively (167-303 W/m2). On the other hand, from the wind energy density verified GWA map, the energy density is found to be 162-293 W/m$^2$ in the Northern nearshore area (Figure 7). Where as in a specified location, it is estimated to have around 511 W/m$^2$ of energy density. Another corner of the map which is situated in the Western coast, the variation of 231-294 W/m$^2$ energy density has been found.

## VI. Test Case

A case study has been performed through assembling all the obtained datasets (ASAR, GWA and ASCAT). Through an engineering application this test case has been approached to estimate an offshore wind park production for an appropriate zone at the Bay of Bengal.

### *A. Selection of the suitable location*

The main focus is to create a 400 MW wind farm at low depth sea locations but high in power density; which is 4-6 km close to the shore, so that it does not require any supplementary base station and additionally, it will reduce the cost of the offshore wind farm installation. The proceeding steps of this engineering application has been displayed in a flowchart below.

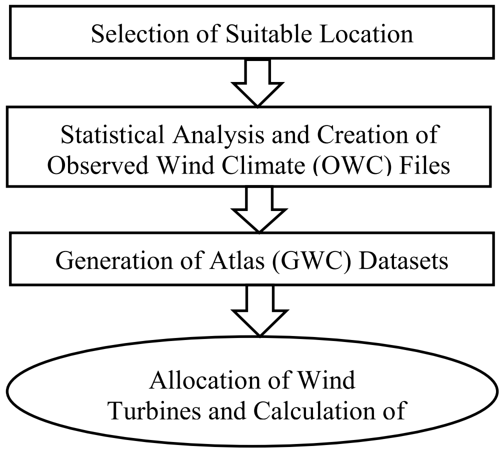


Figure 8. Flowchart of Case Study Phases

Our achieved SAR and GWA power density maps were analyzed to find a comparable higher energy density area comprising higher sample number of SAR dataset. When a point location has more number of SAR samples that represents more data acquisition in the time domain which can lead to a reliable estimation of wind energy density. Also, another preferences were to find a nearshore, lowest depth and highest potential area for case study purpose. To apply the newest technology of offshore wind turbine in the specified area, it leads to operational uncertainty and more expenses. That is why the conventional turbine installation techniques has been preferred in this section.

Therefore, based on four detailed criterion, the zone has been selected as (1) Sufficient number of satellite data sample to get more accurate results. (2) Highest wind energy density region as an aspect to highest energy production. (3) Nearest to shore to not to have a base station in offshore. (4) Lowest depth region to deal with the present technology of the offshore with turbine.

To determine a potential region for wind farm setting, selection of the highest wind energy density location is a must. For this purpose, the attained ASAR based Atlas and GWA power density maps were well analyzed to find out a specific zone with equivalent high power density (fig 9). In order to perform detailed analysis, the sample number of ASAR datasets were prioritized as a purpose of achieving more accuracy in wind energy estimation.

For a purpose of depth analysis of the Bay of Bengal, the bathymetry map has been downloaded in Shuttle Radar Topography Mission (SRTM) 30+ version of 30 arc second, Global. SRTM 3-arc second resolution digital elevation maps (DEM) have been merged with the vector map of the Bay of Bengal and divided in 6 zonal divisions. The target was to focus on the lowest depth zone and near to shore location.

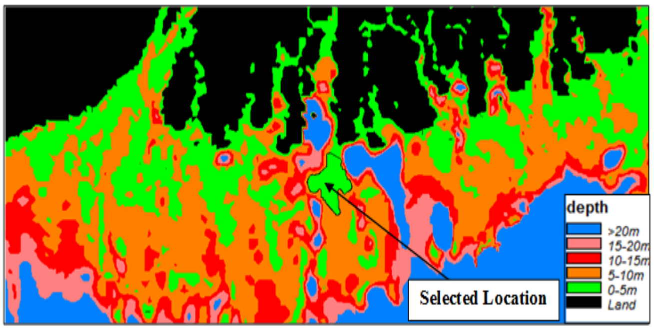

Figure 10. Bathymetrical segmentation of the Bay of Bengal

After investigating the criteria, such close to shore, higher sample number and lower depth areas with higher wind power density was found to be existed only at the northwest coast of Bangladesh. Therefore, the area has been chosen at the location of 21.5° Northern latitude and 88.667° Eastern longitude. This area is in the depth region of 0-5m, 5 km away from the coastline, comprising one of the highest sample numbers of 122 of ASAR datasets and predicted to have higher wind power density in an assumption from GWA and ASAR based wind datasets. In addition, ASCAT dataset was obtained for the chosen area which comprises a full year of 2015 measurements. The dataset contains 567 time series samples that fairly distributed in every single month and ascending-descending arrangement. This obtained ASCAT dataset is more frequent than ASAR datasets due to its technological aspects. Both of the satellite datasets were analyzed accordingly to get a broader interpretation.

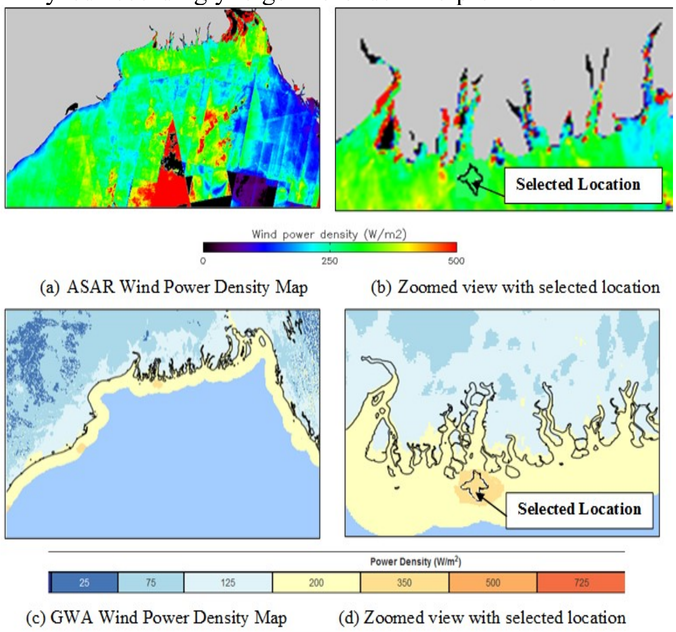

Fig 9. Selection of the suitable location

*B. Implying the statistical analysis*

In our study, we investigated Weibull fitting by 4 methods as Empirical method (EM), Moment Method (MOM), Moment 3 method (MOM 3) and power density method (PDM) in the selected zonal area for wind farm. In addition, the relative accuracy test of Root Mean Square Error (RMSE), Chi-Square ($\chi^2$) and Coefficient of determination ($R^2$) has also performed to predict the energy density uncertainty. Here, it should be mentioned that, RMSE and ($\chi^2$) is considered more accurate when it is near to zero and ($R^2$) is considered more accurate when it is near to its highest value of 1.

| Method | A | k | $v_m$ | RMSE | $\chi^2$ | $R^2$ |
|---|---|---|---|---|---|---|
| EM | 7.39 | 2.09 | 6.54 | 0.0065410 | 0.10419 | 0.88102 |
| MOM | 7.39 | 2.07 | | 0.0065391 | 0.10349 | 0.88108 |
| MOM3 | 7.392 | 2.12 | | 0.0065568 | 0.10615 | 0.88044 |
| Epf | 7.392 | 2.13 | | 0.0065668 | 0.1071 | 0.88007 |

| Method | A | k | $v_m$ | RMSE | $\chi^2$ | $R^2$ |
|---|---|---|---|---|---|---|
| EM | 6.2451 | 2.2107 | 5.5309 | 0.003134 | 0.059732 | 0.91432 |
| MOM | 6.2453 | 2.1950 | | 0.003104 | 0.058549 | 0.91593 |
| MOM3 | 6.2453 | 2.1898 | | 0.003095 | 0.058197 | 0.91643 |
| Epf | 6.2452 | 2.1993 | | 0.003112 | 0.05886 | 0.91549 |

TABLE 1. TWELVE SECTORAL STATISTICAL WEIBULL ANALYSIS OF ASAR DATASETS

TABLE 2.TWELVE SECTORAL STATISTICAL WEIBULL ANALYSIS OF ASCAT DATASET

From the results, the MOM 3 method was chosen to be the best fit for the datasets and further WAsP analysis has been performed to predict the annual energy production of that particular area.

*C.Reformation of Sectoral division*

As the observed dataset of our study did not have efficient sample numbers for each sector, the samples were too few to count, that is why another proposed idea has been represented here. The proposed idea is to obtain more wind speed datasets in one sector, by reforming the sectoral division to 60 degree from 30 degree. So, in spite of having 12 sectors now, 6 sectoral representation has been investigated. As a result, the number of

samples for wind speed calculation increased in every sector and it shows a better result of Weibull fitting.

*D.Wind Farm Layout*

The selective zone was calculated and found to have 174.5 $km^2$. Based on this area, a minimum production from that extent was designed via allocating 134 turbines. These 134 turbines were chosen to have 3MW capacity individually. This results as estimation of 402 MW capacity offshore farm with 2.3 MW/ $km^2$ energy distribution per area. In our study, Vestas V112-3.0 MW model of turbine has been chosen which has a rotor diameter of 112 m and hub height of 84m. As at present, mostly used turbines are of around 3 MW for offshore wind technology, our turbine specification has been chosen accordingly. Turbines were set in an equidistant of 10 diameter from each other as a way to let the wind recover from turbine to turbine.

Turbines front sides were also considered depending on the dominant wind directions. It was found to be 229.459°, 218.015 for ASCAT and ASAR datasets respectively. The dominant direction for every sector has been determined by combining the wind speed and frequency generation of that respective sector and the opposite sector. In the below figure 11 the different wind farm layout based on the leading wind direction is presented where it shows a slight rotation of wind turbines formats.

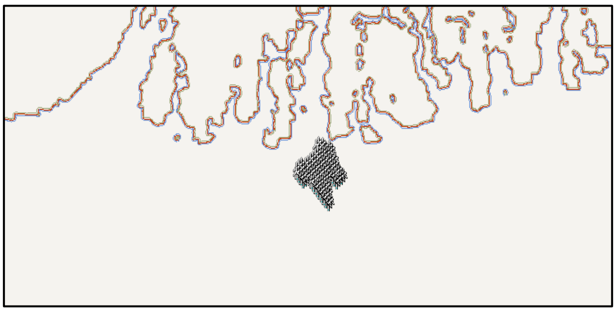

(a) Selected area of turbine allocation

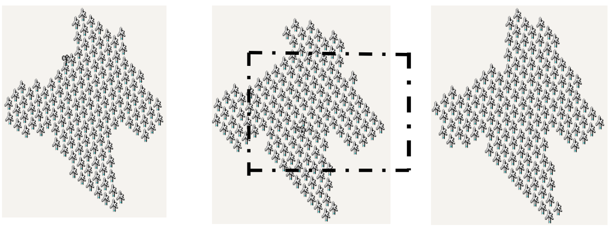

SAR (218.015 °) ASCAT (229.459°) GWA (232.2 °)

(b) Selected location for each datasets

Figure 11. Wind farm layout for every datasets.

*E.Calculation of Annual Wind Energy Production*

After the wind farm insertion to the selective WAsP file, the calculation of Annual Wind Energy has been performed. The gross AEP is the energy production of a single turbine through corresponding wind distribution at the predicted hub height in the form of the supplied power curves. In gross AEP, the wake effect is not accounted. And for Net AEP case, the wake effect is counted as it the whole total annual energy of the farm. By the intricacy of this power curve and numerical wind distribution, each turbines annual energy production is calculated. Afterwards, by combing the each turbines annular energy and wake loses, the AEP is calculated for the whole wind farm.

TABLE 3. CALCULATION OF AEP USING MOMENT 3 METHOD

| Source | Gross AEP (GWh) | Net AEP (GWh) | Wake Loss (%) |
|---|---|---|---|
| ASAR 12 | 1792 | 1693 | 5.52 |
| ASAR 6 | 1793 | 1682 | 6.22 |
| ASCAT 12 | 1385 | 1310 | 5.45 |
| ASCAT 6 | 1379 | 1269 | 7.99 |
| GWA | 1352 | 1276 | 5.61 |

The above table (table 3) shows AEP estimation through MOM 3 method for all three datasets in 5 forms which are- ENVISAT ASAR for 12 sector and 6 sector, ASCAT for 12 sector and 6 sector and GWA. The results are quite similar among ASCAT and GWA, whereas ENVISAT ASAR datasets has an overestimation.

TABLE 4. ERROR CALCULATION OF SATELLITE DATASETS WITH RESPECT TO GWA.

| **Source** | **Sector** | **Error Rate (%)** |
|---|---|---|
| ENVISAT ASAR | 12 | 28 |
| ENVISAT ASAR | 6 | 27.6 |
| ASCAT | 12 | 2.6 |
| ASCAT | 6 | 0.5 |

While comparing the 12 sectors, it estimates a higher NET AEP, which leads to a higher error rate compared with GWA (table 4). On the other hand, when the sectors are enlarged (from 12 sector to 6 sectors), the error rate is less specially in ASCAT scenario. But the wake losses are found to be in rise when it is 6 sector

## VIII. CONCLUSION

For a large offshore area, it is very difficult to define where should be focused on for planning of an offshore windfarm. Even we know, satellite measurements are new and has limited number of samples in any location, they are still the only representative of onsite measurements more than any of the models. Several models of satellites along with its higher number of samples can be used without any local measurements, although this can lead to very big uncertainties. But it can estimate a general region for further broad investigation.

Consequently, in this paper three (ENVISAT ASAR, ASCAT and GWA) remote sensing measurements have been discussed and those datasets were used primarily to generate a wind Atlas of the Bay of Bengal and by utilizing that Atlas a potential zone has been found at a near shore area of the Bay of Bengal. Formerly, a case study has been performed to predict the Annual Energy Production of that particular area. Among these datasets, two (ENVISAT ASAR and ASCAT) are from satellite based and one (GWA) from long term mesoscale model measurement. The satellite datasets were compared with GWA, as no offshore wind farm has been established in the Bay of Bengal yet and there is no onsite data to have a suitable comparative study.

The resulted calculation with their error is pointing towards the fact of directional view of wind (sectors) and lesser number of samples. Differences were accounted because of limited data in some sectors. So, reducing number of the sectors were suggested which showed improvement in Weibull fitting, though it has a slight increase in wake effects. Analysis shows that while there is not enough samples, all the methods shows similar results. One can understand from this result that, satellite data can be used to identify the highest density areas for a particular zone but it cannot be used exactly to estimate the highest region. As in our study, the satellite datasets were pointing the same location with GWA and one can make a preliminary analysis of the wind conditions by knowing that it can go up to 20% uncertainty.

From this paper, it can be said that, satellite gives us the ability to identify the higher power density area so that we can utilize it for met mast set up. Even to find a potential zone for establishing mat mast is challenging and time worthy. The foundation of this thesis project is that, satellite datasets can be used to identify potential zone and it has a promising outcome of calculation capability of annual energy production, if compared with any long time statistical result and bathymetry data combination. Furthermore, all three datasets used in this study comprises similar AEP (ASCAT better than ASAR) at the coastal area which indicates the selective location as a potential area and further researches regarding this study can lead towards a better future for the wind energy sector of Bangladesh.

## REFERENCES

[1] Beaucage, P., Bernier, M., Lafrance, G., & Choisnard, J. (2008). Regional mapping of the offshore wind resource: Towards a significant contribution from space-borne synthetic aperture radars. IEEE Journal of Selected Topics in Applied Earth Observations and Remote Sensing, 1(1), 48-56.

[2] Kader, A., Chowdhury, M. Z. R., Uddin, M. M., Hoque, M. E., & et al. Bathymetric study of the Bay of Bengal based on open source satellite and sounding data. International Journal of Geomatics and Geosciences, 4(1), 116.

[3] Christiansen, M. B. (2006). Wind energy applications of synthetic aperture radar. Institute of Geography, Faculty of Science, University of Copenhagen.

[4] Dagestad, K.-F., Horstmann, J., Mouche, A., Perrie, W., Shen, H., Zhang, B., Lehner, S. (2012). Wind retrieval from synthetic aperture radar-an overview. Paper presented at the 4th SAR Oceanography Workshop (SEASAR 2012).

[5] Hasager, C. B., Mouche, A., Badger, M., Bingöl, F., Karagali, I., Driesenaar, T., Longépé, N. (2015). Offshore wind climatology based on synergetic use of Envisat ASAR, ASCAT and QuikSCAT. Remote Sensing of Environment, 156, 247-263.

[6] Hasager, C. B., Astrup, P., Christiansen, M. B., Nielsen, M., & Barthelmie, R. (2006). Wind resources and wind farm wake effects offshore observed from satellite. Paper presented at the Proceedings of the European Wind Energy Conference and Exhibition (EWEC).

[7] Ricciardulli, L., Wentz, F.J. (Producer). (April 2016, 20 June, 2016). Remote Sensing Systems ASCAT C-2015 Daily Ocean Vector Winds on 0.25 deg grid, Version 02.1. Retrieved from www.remss.com/missions/ascat

[8] Hasager, C. B., Bingöl, F., Badger, M., Karagali, I., & Sreevalsan, E. (2011). Offshore Wind Potential in South India from Synthetic Aperture Radar (8755039081). Retrieved from http://orbit.dtu.dk/fedora/objects/orbit:87302/datastreams/file_7749647/content

[9] Hasager, C. B., Mouche, A., Badger, M., Bingöl, F., Karagali, I., Driesenaar, T. Longépé, N. (2015). Offshore wind climatology based on synergetic use of Envisat ASAR, ASCAT and QuikSCAT. Remote Sensing of Environment, 156, 247-263.

[10] Peña, A., Hahmann, A., Hasager, C. B., Bingöl, F., Karagali, I., Badger, J.,Clausen, N.-E. (2011). South Baltic Wind Atlas: South Baltic Offshore Wind Energy Regions Project: Risø DTU-National Laboratory for Sustainable Energy.

[11] Bingöl, F., Hassager, C. B., Badger, M., & Badger, J. (2013). RZGM2013-14.

[12] Global Wind Atlas. (2015). Retrieved from http://globalwindatlas.com/tutorials.html

[13] Hasager, C. B., Astrup, P., Barthelmie, R., Dellwik, E., Mortensen, N. G., Nielsen, M Rathmann, O. (2002).

[14] ASCAT, Metop Meteorological Missions. (2006). Retrieved 28 June 2016, from European Space Agency (ESA),Retrieve from http://www.esa.int/Our_Activities/Observing_the_Earth/The Living_Planet_Programme/Meteorological_missions/MetO

[15]SAF, O. (2013). ASCAT Wind Product User Manual. Version, 1, 23.

[16] Kidmo, D., Danwe, R., Doka, S., & Djongyang, N. (2015). Statistical analysis of wind speed distribution based on six Weibull Methods for wind power evaluation in Garoua, Cameroon. Revue des Energies Renouvelables, 18(1), 105-125

[17] Amaya-Martínez, P.-A., Saavedra-Montes, A.-J., & Arango-Zuluaga, E.-I. (2014). A statistical analysis of wind speed distribution models in the aburrá valley, Colombia. CT&F-Ciencia, Tecnología y Futuro, 5(5), 121-136